

Van der Waals Density Functional for Layered Structures

H. Rydberg,¹ M. Dion,² N. Jacobson,¹ E. Schröder,¹
 P. Hyldgaard,¹ S.I. Simak,¹ D.C. Langreth,² and B.I. Lundqvist^{1,*}

¹ *Department of Applied Physics, Chalmers University of Technology and Göteborg University, SE-412 96 Göteborg, Sweden*

² *Center for Materials Theory, Department of Physics and Astronomy,
 Rutgers University, Piscataway, New Jersey 08854-8019*

(Dated: August 6, 2003)

To understand sparse systems we must account for both strong local atom bonds and weak nonlocal van der Waals forces between atoms separated by empty space. A fully nonlocal functional form [H. Rydberg, B.I. Lundqvist, D.C. Langreth, and M. Dion, Phys. Rev. B **62**, 6997 (2000)] of density-functional theory (DFT) is applied here to the layered systems graphite, boron nitride, and molybdenum sulfide to compute bond lengths, binding energies, and compressibilities. These key examples show that the DFT with the generalized-gradient approximation does not apply for calculating properties of sparse matter, while use of the fully nonlocal version appears to be one way to proceed.

PACS numbers: 71.15.Mb, 61.50.Lt, 31.15.Ew, 73.21.-b

Calculations of structure and other properties of sparse systems must account for *both* strong local atom bonds *and* weak nonlocal van der Waals (vdW) forces between atoms separated by empty space. Present methods are unable to describe the true interactions of sparse systems, abundant among materials and molecules. Key systems, like graphite, BN, and MoS₂, have layered structures. While today's standard tool, density-functional theory (DFT), has broad application, the common local (LDA) and semilocal density approximations (GGA) [1, 2, 3, 4] for exchange and correlation, $E_{xc}[n]$, fail to describe the interactions at sparse electron densities. Here we show that the recently proposed density functional [5] with nonlocal correlations, $E_c^{nl}[n]$, gives separations, binding energies, and compressibilities of these layered systems in fair agreement with experiment. This planar case bears on the development of vdW density functionals for general geometries [6, 7], as do asymptotic vdW functionals [8].

Figure 1 with its 'inner surfaces' defines the problem: voids of ultra-low density, across which electrostatics leads to vdW coupling. This coupling depends on the polarization properties of the layers themselves, and *not* on small regions of density overlap between the layers, excluding proper account in LDA or GGA. For large interplanar separation d the vdW interaction energy between planes behaves as $-c_4/d^4$, while LDA or GGA necessarily predicts an exponential falloff. Layers rolled up to form two (i) nanotubes with parallel axes a distance l apart interact as $-c_5/l^5$, or (ii) balls (*e.g.*, C₆₀), a distance r apart, as $-c_6/r^6$. If by fluke an LDA or GGA were to give the correct equilibrium for one shape, it would necessarily fail for the others. The simple expedient of adding the standard asymptotic vdW energies as corrections to the correlation energy of LDA or GGA also fails. The true vdW interaction between two close sheets must be (i) substantially stronger (Fig. 1), (ii) *seamless*, and (iii)

saturate as d shrinks (Fig. 2).

Like earlier work directly calculating nonlocal correlations between two jellium slabs [9], the vdW density functional (vdW-DF) theory [5] used here exploits assumed planar symmetry. It divides the correlation energy functional into two pieces, $E_c[n] = E_c^0[n] + E_c^{nl}[n]$, where $E_c^{nl}[n]$ is defined to include the longest ranged or most nonlocal terms that give the vdW interaction and to approach zero in the limit of a slowly varying density. The term $E_c^0[n]$ is also nonlocal, but approaches the LDA in this limit. The two terms are approximated differently. Here the LDA is used for $E_c^0[n]$, as the LDA should be much more accurate with the principal longest range terms separated off. Ultimately we plan to derive a gradient or GGA expansion appropriate to $E_c^0[n]$, but the resulting corrections are expected to be small. Thus we use

$$E_c[n] \approx E_c^{LDA}[n] + E_c^{nl}[n]. \quad (1)$$

Long range terms are less sensitive to details of the system's dielectric response. Thus very simple approximations for the dielectric function are made for $E_c^{nl}[n]$. We care to make the polarization properties of a single layer come out reasonably.

For systems with planar symmetry, the predominant component of the nonlocal correlation energy E_c^{nl} giving the vdW forces can be determined simply by comparing the solutions of the Poisson equation $\nabla \cdot (\epsilon \nabla \Phi) = 0$ and the Laplace equation $\nabla^2 \Phi = 0$ [5]. The crux of the approximation is the use of a simple plasmon-pole model for the dielectric function,

$$\epsilon_k(z, iu) = 1 + \frac{\omega_p^2(z)}{u^2 + (v_F(z)q_k)^2/3 + q_k^4/4}, \quad (2)$$

where $\omega_p^2(z) = 4\pi n(z)e^2/m$, and $mv_F(z) = (3\pi^2 n(z))^{1/3}$ are functions of the local density $n(z)$. The 2D wave

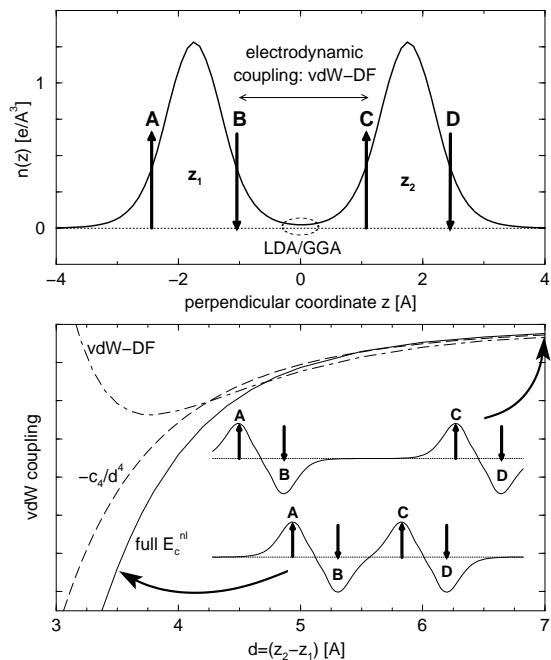


FIG. 1: Schematics of the vdW forces in sparse, layered materials. *Top panel*: Laterally averaged electron-density profile of two graphene layers at equilibrium separation $d \approx 3.5$ Å. The dotted ellipse indicates the region determining the interlayer interaction within LDA or GGA. It is unable to describe the true long range interaction (horizontal arrow) between correlated charge fluctuations (extrema illustrated by those of the finite-frequency charge response, and labelled by vertical arrows). *Bottom panel*: Full E_c^{nl} (solid curve) vs. the asymptotic form of $E_c^{nl} \rightarrow -c_4/d^4$ (dashed line). Also shown: full ground state interaction energy (dash-dotted line). *Insets*: Sketches of the correlated charge fluctuations for different layer separations, explaining why $|E_c^{nl}| > c_4/d^4$. In the asymptotic region (top inset), attractive interactions BC and AD are nearly cancelled by the repulsive interactions AC and BD, leaving little more than the weak dipolar interaction. Near equilibrium separation (bottom inset), the repulsive interactions AC and BD remain specified by the layer separation d , but the relative strengthening of attractive interaction BC substantially overcompensates the relative weakening of the attractive interaction AD. At still smaller d , E_c^{nl} becomes weaker and saturates (Fig. 2, inset).

vector perpendicular to the z direction is \mathbf{k} , iu is the imaginary frequency and $q_k^2 = k^2 + q_\perp^2$ mimicks the 3D wave vector, with the z direction accounted for by the $n(z)$ dependence and q_\perp taken as a constant.

Our scheme, applied to jellium surfaces in Ref. 5, is used here for layered systems, for simplicity a two-layered system (*e.g.*, two parallel graphene sheets) arranged perpendicular to the z axis, at positions $z = 0$ and $z = d$, respectively. The first step is to calculate the density in DFT with a suitable approximation, which we take to be an appropriate flavor of the GGA, and to average it in the lateral direction to yield $n(z)$. The next two steps represent the key to the success of our approximation.

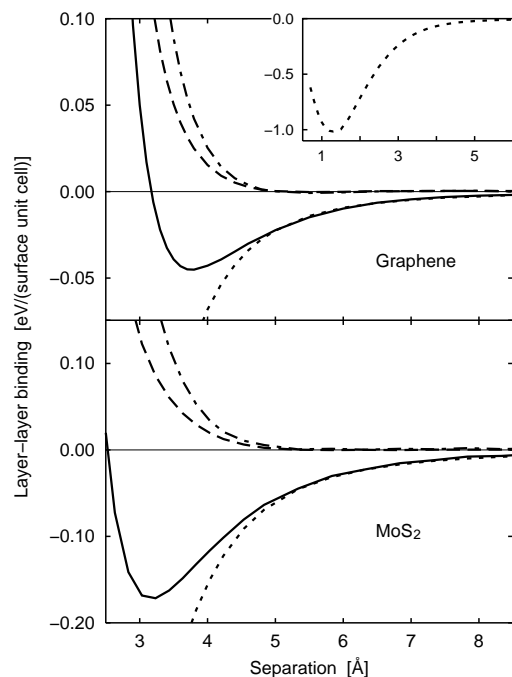


FIG. 2: Calculated vdW-DF results for the interlayer binding (adhesion) between two sheets of graphene (*upper panel*) and MoS₂ (*lower panel*) as functions of the interlayer separation d . In each panel it is compared (solid curves) with the underlying GGA (dashed curves), and with the adhesion *in the absence* of the vdW-DF term E_c^{nl} (dash-dotted curves) calculated using only the first two terms of Eq. (5) for E_{xc} . The nonlocal-correlation vdW contribution E_c^{nl} alone is shown separately (dotted curves). The figure shows that no binding results from exchange or local correlation; the vdW interactions provides adhesion in fair agreement with experiment (Table I). The *inset* shows that our calculated value of E_c^{nl} saturates for small d values.

First one calculates from first principles the perpendicular static polarizability α of a *single* layer of the material (a graphene layer in this example) in the ground-state DFT scheme with the above GGA flavor. Then one fixes the constant q_\perp so that dielectric model (2) gives precisely the same polarizability, that is

$$\alpha = \frac{1}{4\pi} \int dz \left[1 - \frac{1}{\epsilon_0(z, 0)} \right]. \quad (3)$$

This step mitigates the errors introduced both by the lateral averaging and the dielectric model. The leading vdW interaction is proportional to an integral over the square of the dynamic polarizabilities. Previous work in the asymptotic limit [8] shows that simple, properly scaled dielectric functions giving the correct static polarizabilities form good approximations to the dynamic ones, hence giving accurate vdW interactions.

The correlation energy can be calculated from the charge response [10]. With planar symmetry only the response to an arbitrarily charged sheet $\rho \propto \exp(i\mathbf{k} \cdot$

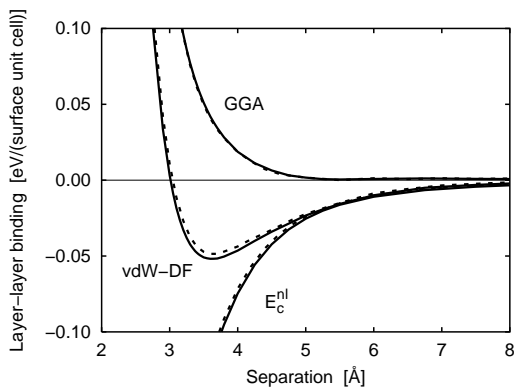


FIG. 3: Comparison of the vdW-DF layer-to-layer binding in the staggered bulk hexagonal-BN system (solid lines) and adhesion between two sheets of BN (broken lines) shown as functions of the interlayer separation $d = c/2$. In both descriptions the GGA gives unphysical results for bond and equilibrium separation. The total adhesion is dominated by the contribution of the vdW interaction E_c^{nl} . The nearest-neighbor interlayer binding (broken lines) is seen to strongly dominate the bulk adhesion (solid lines) for layered materials.

$\mathbf{r})\delta(z - z_-)$ placed at an offset z_- ($z_- \ll 0$) from one end of the sample needs to be calculated. Integrating Poisson's equation with ϵ as in (2) one finds the z component of the electric field $E_z(z_+)$ at $z = z_+ \gg d$. Then E_c^{nl} is given by [5]

$$E_c^{\text{nl}} = -A \int_0^\infty \frac{du}{2\pi} \int \frac{d^2k}{(2\pi)^2} \ln \frac{E_z(z_+)}{E_z^0(z_+)}, \quad (4)$$

where A is the lateral area and $E_z^0(z_+)$ is the electric field component from the charge sheet at $z = z_-$ in the absence of the sample. In Eq. (4) the spatial dependences of the two E 's cancel in the ratio, leaving only the k dependence. For each of the bulk solids considered here we apply this method to 32 and 30 layer slabs to give, by subtraction, a well converged per layer value of E_c^{nl} .

The approximation for the exchange energy functional $E_x[n]$ should be consistent with our approximation for $E_c^0[n]$, that is a local or semilocal one. We use a version that best approximates exact density functional exchange, namely Zhang and Yang's [3] (ZY) "revPBE" exchange functional $E_x^{\text{ZY}}[n]$, where the parameter controlling the large gradient limit in the PBE exchange functional [2] is fitted to exact density-functional exchange calculations. Unlike exchange [11] in PW91 [1], PBE [2], and RPBE [4], E_x^{ZY} shows no tendency to bind any of the vdW systems we have tried it on, unless the vdW correlation is actually included in the calculation. We thus take

$$E_{\text{xc}}[n] = E_x^{\text{ZY}}[n] + E_c^{\text{LDA}}[n] + E_c^{\text{nl}}[n]. \quad (5)$$

The first two terms form an important and recommended starting point for testing nonlocal vdW functionals. They

TABLE I: Properties of graphite, BN, and MoS₂, calculated with vdW-DF and compared to experimental data in parentheses, when available. The table shows the geometry (a, c), binding energy (E_0), bulk modulus (B_0), and elastic constant (C_{33}). GGA (not shown) binds very weakly at unphysically large c or not at all, depending on substance and GGA flavor.

	Graphite	BN	MoS ₂
a [Å]	2.47 (2.46) ^a	2.51 (2.50) ^b	3.23 (3.160) ^c
c [Å]	7.52 (6.70) ^d	7.26 (6.66) ^b	12.6 (12.29) ^c
E_0 [meV/at]	24 (35 ± 10) ^e	26	60
B_0 [GPa]	12 (~33) ^a	11	39
C_{33} [GPa]	13 (37-41) ^a	11	49

^aRef. 23.

^bRef. 24.

^cRef. 25.

^dRef. 26.

^eRef. 27.

assure a vdW attraction that actually comes from terms that in principle are capable of giving it.

The GGA is used in order to have a good account of strong valence bonds and densities of individual layers, and the above scheme is implemented by self-consistently calculating the energy E^{GGA} and density n^{GGA} , typically in the revPBE flavor of GGA. The total energy, as a function of the lattice parameters, is then calculated as $E \approx E^{\text{GGA}}[n^{\text{GGA}}] + \Delta[n^{\text{GGA}}]$, where $\Delta[n] = E_c^{\text{nl}}[n] - E_c^{\text{grad}}[n]$ and $E_c^{\text{grad}}[n] = E_c^{\text{GGA}}[n] - E_c^{\text{LDA}}[n]$. This approximation treats Δ as a post GGA perturbation. The GGA calculations are done using the plane-wave pseudopotential [12] DFT code dacapo [13].

The three materials considered here have layered structures with a soft direction perpendicular to the layers [14]. Strong covalent bonds occur between the atoms within the hexagonal layers (lattice constant a), while weak vdW interactions occur between the layers. Graphite has a staggered or A-B type stacking with the intralayer C atoms in regular, planar hexagons stacked with corners on top of centers. Boron nitride, isoelectronic with graphite, has no shift in hexagon locations but B and N atoms in alternate positions along the c -direction. A similar alternation occurs between Mo and S atoms in the A-B type structure of MoS₂ [15].

Calculations are also performed for bilayers of the three systems. The binding-energy curve of two parallel graphene sheets [16], *i.e.* the total-energy difference at separation d and at infinite separation, respectively, for varying d (Fig. 2) gives in the approximation [5] with vdW-DF, Eq. (5), a close relation to experimental findings for binding energy and equilibrium distance. The GGA curve, on the other hand, is completely wrong, which we blame on absence of vdW effects. The inset shows that our E_c^{nl} contribution gives stronger binding than the traditional asymptotic vdW interaction. The

binding-energy curve for two parallel BN sheets (Fig. 3) differs little from that of bulk BN as a function of lattice constant c . At equilibrium the calculated E_c^{nl} difference is $\sim 4\%$, attributable mostly to 2nd nearest layers in the bulk material [17].

Bulk-modulus values are computed together with other structure (a, c) and bonding properties [18] (Table I). It is crucial to densely sample the region of (a, c) values around the optimal structure (a_0, c_0), and we use a new method [19] for direct evaluation of both structure, binding energy, and bulk modulus B_0 in the relevant range of a and c values [20]. GGA values were also computed but not shown. For all three materials the various GGA flavors give no binding or bind very weakly at unreasonably large separation. The vdW-DF, on the other hand, gives values for lattice parameters and cohesive energy in good agreement and for bulk modulus in fair agreement with experimental values, when available.

In conclusion, we recommend the replacement of GGA as a standard method in total-energy calculations with vdW-DF as given in Eq. (5) for descriptions of layered systems that contain sparse electron distributions. This will give the right qualitative character of soft bonds, including saturation of the vdW potential at small separations, and even quantitative ones, like physical values of bond lengths, binding energies, and compressibilities [28].

We are grateful to K. W. Jacobsen for suggesting tests on MoS₂ layers [21]. Financial support from the Swedish Foundation for Strategic Research via Materials Consortia #9 and ATOMICS, STINT, and the Swedish Scientific Council are gratefully acknowledged. Work by M.D. and D.C.L. supported in part by NSF Grant DMR 00-93070.

* To whom correspondence should be addressed; E-mail: lundqvist@fy.chalmers.se.

- [1] J. P. Perdew *et al.*, Phys. Rev. B **46**, 6671 (1992); **48**, 4978(E) (1993).
- [2] J. P. Perdew, K. Burke, and M. Ernzerhof, Phys. Rev. Lett. **77**, 3865 (1996).
- [3] Y. Zhang and W. Yang, Phys. Rev. Lett. **80**, 890 (1998).
- [4] B. Hammer, L. B. Hansen, and J. K. Nørskov, Phys. Rev. B **59**, 7413 (1999).
- [5] H. Rydberg, B. I. Lundqvist, D. C. Langreth, M. Dion, Phys. Rev. B **62**, 6997 (2000).
- [6] H. Rydberg, Ph D. Thesis (2001), Chalmers ISBN 91-7291-068-2.
- [7] M. Dion, H. Rydberg, B. I. Lundqvist, and D. C. Langreth, to be published.
- [8] See E. Hult, P. Hyldgaard, J. Rossmeisl, and B. I. Lundqvist, Phys. Rev. B **64**, 195414 (2001) and E. Hult, H. Rydberg, B. I. Lundqvist, D. C. Langreth, Phys. Rev. B **59**, 4708 (1998), and references therein.
- [9] J. F. Dobson and J. Wang, Phys. Rev. Lett. **82**, 2123 (1999).
- [10] The coupling constant integration in E^{nl} is performed via the following approximation: $\epsilon - 1 \approx \lambda[(\epsilon - 1)/\lambda]_{\lambda=1}$. This approximation gives the long range van der Waals interaction exactly [7] for dielectric functions of the type used here. The λ dependence comes via q_{\perp} .
- [11] Y. Zhang, W. Pan, and Y. Yang, J. Chem. Phys. **107**, 7921 (1997); X. Wu *et al.*, J. Chem. Phys. **115**, 8748 (2001).
- [12] Only the valence density was used in the functional, because the lateral averaging unphysically lowers the core density and increases the size of the core, yielding an unphysically large vdW contribution. Nevertheless, tests with the full density showed negligible effect on the geometry, and at most a 30% increase in well depth.
- [13] <http://www.fysik.dtu.dk/CAMPOS/>.
- [14] Separation $d = c/2$, except for MoS₂, where d is defined as the distance from the perpendicular position of the top-most sulfur atom of one layer to the position of the bottom-most sulfur atom of the next.
- [15] In the MoS₂ interlayer calculations, each MoS₂ layer is treated as a composite material (the Mo-S perpendicular separation is ~ 1.58 Å). A composite q_{\perp} value (~ 0.58), identical in both MoS₂ layers, is obtained by applying an external field across a single MoS₂ composite and using GGA to calculate the static polarization. In the interaction study the vdW-DF energy is then calculated as a function of the separation between the two MoS₂-layer composite materials, the atom positions within each of the MoS₂-layer composites being kept fixed.
- [16] M. S. Dresselhaus *et al.*, *Graphite Fibers and Filaments* (Springer, Berlin, 1988).
- [17] The 4% figure may be estimated as $1/(1.5 \times 2^4)$, with the divisor of 1.5 occurring because the 50% enhancement (Fig. 1) is not applicable at the 2nd layer distance.
- [18] Using $E_{\text{vdW-DF}}(c, a) = E_{\text{GGA}}(c, a) + \Delta(c, a) - \Delta(\infty, a)$.
- [19] E. Ziambaras and E. Schröder, Phys. Rev. B, in press, cond-mat/0304075.
- [20] The value of 33 GPa reported earlier [22] was incorrect.
- [21] M. V. Bollinger *et al.*, Phys. Rev. Lett. **87**, 196803 (2001); M. V. Bollinger, K. W. Jacobsen, and J. K. Nørskov, Phys. Rev. B **67**, 085410 (2003).
- [22] H. Rydberg, *et al.*, Surf. Sci. **532-535**, 606 (2003).
- [23] *Landolt-Börnstein search* (Springer, Berlin, 2003), <http://link.springer.de>.
- [24] G. Kern, G. Kresse, and J. Hafner, Phys. Rev. B **59**, 8551 (1999).
- [25] Th. Böker *et al.*, Phys. Rev. B **64**, 235305 (2001).
- [26] Y. Baskin and L. Mayer, Phys. Rev. **100**, 544 (1955).
- [27] L. X. Benedict *et al.*, Chem. Phys. Lett. **286**, 490 (1998).
- [28] Future work that may remove the remaining differences includes (i) time dependent DFT and other calculations of the positions of the polarization peaks (Fig. 1) followed by improvements to the approximation Eq. (2), (ii) derivation of the gradient corrections appropriate to E_c^0 with corresponding modifications to Eq. (1), and (iii) implementation of exact exchange with corresponding modifications to Eq. (5).